COMPARISON OF SUPERCRITICAL AND DISSOLVED CO_2 INJECTION SCHEMES

Catherine Ruprecht and Ronald Falta

Clemson University, Department of Environmental Engineering and Earth Sciences, Brackett Hall 340C, Clemson, SC 29634-0919, USA
e-mail: cruprec@clemson.edu; faltar@clemson.edu

ABSTRACT

The distribution of CO_2 in a storage formation following injection is highly relevant to the risk to drinking water aquifers potentially posed by geological carbon sequestration. Understanding where the injected CO_2 is likely to migrate in the storage formation helps anticipate possible failure modes for the injected fluids. Supercritical CO_2 injection and CO_2 saturated- brine injection have been chosen for investigation in the current work.

Results show that the areal footprint of supercritical CO_2 is initially close to half the size of the dissolved CO_2, independent of formation heterogeneity. Following injection, supercritical CO_2 remains highly mobile, buoyantly flowing upward and significantly extending outwards along the sealing layer; whereas dissolved CO_2 slowly sinks, essentially immobilized following injection. Additionally, dissolved CO_2 distributes more uniformly throughout the storage formation in cases of simple and complex formation heterogeneity. These results indicate that dissolved CO_2 injection may reduce the potential for unwanted release from storage.

INTRODUCTION

There are several proposed methods for CO_2 injection into saline aquifers. The CO_2 may be injected as a supercritical phase (Ennis-King and Paterson, 2002), as CO_2 saturated water (Eke, 2009), as brine alternating CO_2 cycles (Eke et al., 2009), as brine and CO_2 co-injection (Qi, 2007; Qi, 2008), or as a CO_2 saturated brine (Lake, 1989, Burton and Bryant, 2007; Eke et al., 2009, Fang et al., 2010, Jain and Bryant, 2011). These methods seek to immobilize stored CO_2 via structural, residual, or dissolved phase trapping mechanisms (Tao and Bryant, 2012).

In this paper, supercritical and brine-saturated injection strategies are compared in order to determine effects on migration and immobilization of CO_2. Comparisons are made between areal extents of the CO_2 plumes and how the storage volume is utilized, in simulation cases of increasing formation heterogeneity. Plume mobilities are compared during a monitoring period following injection, as are the pressure elevations of the different injection strategies.

BACKGROUND

The prevailing technique for CO_2 injection is in the supercritical phase. This method optimizes the mass of CO_2 injected by volume. In this phase, there is a density difference near 300 kg/m^3 between the CO_2 and resident brine. This density difference drives a buoyant migration of CO_2 upward toward the sealing layer (Bachu, 2002; Eke et al., 2009; Benson et al., 2005). Ideally, the seal would have low permeability and high capillary entry pressure. These properties would then act as a barrier and cause the CO_2 to migrate laterally. Due to lower density and viscosity compared to brine, this buoyant, supercritical CO_2 has a tendency to produce viscous and gravitational instabilities upon injection (Garcia and Pruess, 2003; Yamamoto and Doughty, 2011). These hydrodynamic instabilities may lead to pore space bypassing and reduced sweep efficiency (Garcia, 2003). Previous simulation studies have implied that only 2% of the available pore volume will contain CO_2 if it is injected alone (Fang et al., 2010).

Ex situ dissolution is achieved through surface mixing of CO_2 and brine within a pipeline operating at the storage formation's pressure (Leonenko, 2007). This brine is retrieved from the formation via production wells and re-injected once saturated with CO_2. Surface dissolution of the CO_2 in brine changes the mechanics of flow in the subsurface upon injection. Complications associated with saturation fronts, mobility contrasts, viscous fingering, and

reduced phase permeabilities are eliminated (Burton and Bryant, 2007). This single-phase flow leads to a more uniform sweep of the reservoir (Eke et al., 2009; Fang et al., 2010). The solution will tend to sink as a result of slight density differences with the native brine, removing the need for a perfect seal and allowing safe injection at shallower depths (Fang et al., 2010). Additionally, brine production wells may be used to mitigate pressure elevations during injection and regulate the direction of plume flow and displacement of native brine (Leonenko, 2007; Jain and Bryant, 2011; Tao and Bryant, 2012).

SIMULATION METHODS

Regional-scale multiphase flow models are created using Lawrence Berkeley National Lab's TOUGH2-ECO2N to simulate both supercritical and dissolved CO_2 injection into deep saline aquifers. The first set of models represents a homogeneous formation. The second set of models depicts a stratified heterogeneous formation. The third set of models incorporates heterogeneous, random, spatially correlated permeability fields generated from Lawrence Berkeley National Lab's iTOUGH2-GSLIB. The resultant storage formation is highly heterogeneous in all directions, representing a more realistic permeability distribution. A simple history-dependent nonwetting phase trapping model is incorporated into relative permeability and capillary pressure subroutines of TOUGH2-ECO2N.

Model parameters and hydrogeologic characteristics are held constant between comparisons. The same mass of CO_2 is injected in each case; therefore, a much greater total mass (brine plus CO_2) is injected for the dissolved CO_2 case. To accommodate for the resulting pressure increase, injection schemes are designed so as not to exceed the fracture pressure of the formations.

HOMOGENEOUS FORMATION

A preliminary understanding of supercritical and dissolved CO_2 injection strategies is achieved through comparison of storage in a homogeneous formation.

Model Setup

In initial models, a 200 m thick homogenous storage formation is represented using a radial grid refined around the injection well and extending out 200 km. Pressure and temperature gradients are established between the bottom of the storage formation at 20 MPa and 42ºC and the top at 18 MPa and 40.2ºC. All models are run isothermally. The formation is uniformly given a salinity of 50,000 mg/L. The van Genuchten-Mualem Model is chosen to represent the relative permeability of the liquid phase. A scaled cubic function incorporating a simple history-dependent nonwetting phase trapping model is chosen for the gas phase. The van Genuchten function is used for capillary pressure curves, again incorporating a history-dependent nonwetting phase-trapping model.

Relevant hydrogeologic properties of the storage formation and saturation curve parameters are given in Table 1. Parameter values are determined from Birkholzer et al. (2008), Barnes et al. (2009), and Zhou et al. (2010). These values are characteristic of the deep saline aquifers under consideration for carbon capture and storage activities.

Table 1. Hydrogeologic properties of the homogenous storage formation.

Property		
Porosity	ϕ	0.17
Horizontal permeability	k_r	100 md
Vertical permeability	k_z	10 md
Pore compressibility	β_p	3.71 Pa^{-1}
Relative permeability parameters		
Residual brine saturation	S_{lr}	0.3
Van Genuchten parameter	m	0.41
Max. residual CO_2 saturation	S_{gr}	0.25
Capillary pressure parameters		
Capillary entry pressure	α^{-1}	$4x10^3$ Pa
van Genuchten parameter	m	0.41

Injection is conducted for a 20-year period at approximately 160 Mt/yr of CO_2. The rate of CO_2 injected was chosen so pressure elevations due to injection from any one well would not exceed the fracture pressure of the storage formation, set at 3.17 MPa above hydrostatic pressure. In the case of CO_2 dissolved in brine, the brine is assumed to have the same composition as the resident fluid. At the given pressures

and temperatures, a volume of brine approximately 20 times that of the CO_2 is needed for full dissolution. In order to consider long-term storage security, mobility of both phases is compared during a 25-year monitoring period following injection.

Results

Figure 1 shows the CO_2 fronts at the end of 20-year injection periods. Considering a CO_2 mass fraction of 0.005 as the cutoff, the farthest the supercritical CO_2 travels from the well is 415 m along the caprock. The dissolved CO_2 travels more uniformly, flushing the aquifer 920 m from injection.

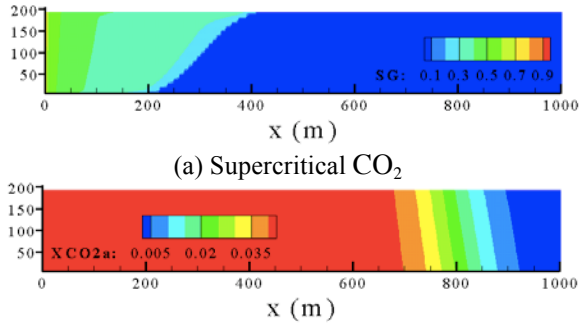

(a) Supercritical CO_2

(b) Dissolved CO_2

Figure 1. The top cross section shows the radial distribution of supercritical CO_2 saturation after 20 years of injection. The bottom cross section shows distribution of the mass fraction of CO_2 in the aqueous phase.

Maximum pressures are achieved at the end of injection in gridblocks along the top of the storage formation closest to the well. These pressures are determined without considering brine production wells elsewhere in the target region. In the supercritical case, the largest pressure increase is 0.60 MPa and in the dissolved case it is at 7.27 MPa. Extents of pressure effects are determined with pressure increase cutoff at 10.0 kPa, or the equivalent of 1 m hydraulic head rise. An elevation in pressure is calculated 24 km from injection in the supercritical CO_2 case and 83 km from injection in the dissolved CO_2 injection case.

Figure 2 shows the distribution of CO_2 80 years after the end of the injection period. Buoyancy and viscous forces drive the supercritical CO_2 to the top of the formation and 550 m from the well. This behavior is an example of gravity override (Yamamoto and Doughty, 2011), which enables CO_2 mobility after injection has stopped. The dissolved CO_2 travels 930 m from the injection well, sinking due to a higher density compared to the resident brine.

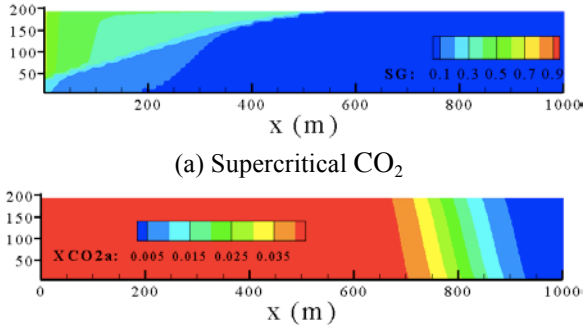

(a) Supercritical CO_2

(b) Dissolved CO_2

Figure 2. The top cross section shows the radial distribution of supercritical CO_2 saturation after 20 years of injection. The bottom cross section shows distribution of the mass fraction of CO_2 in the aqueous phase.

Notably, the dissolved CO_2 sinks to the bottom of the aquifer more slowly than the supercritical CO_2 rises to the top. In the years following injection, it can be seen from these simple models that supercritical CO_2 increases its areal footprint on the cap rock significantly, reducing storage efficiency. Dissolved CO_2 is essentially immobile during this time.

STACKED FORMATION

CO_2 injection into a geology characterized by alternating, laterally extensive layers of higher and lower permeability is anticipated to increase storage security.

Model Setup

In order to simulate this type of geology, a 2 km thick, 200 km radial model is developed. At the base of the model is a storage formation that contains 8 layers of alternating aquifer material. From the storage formation to surface, a stacked system of 12 aquifers and confining units is modeled. Figure 3 shows an image of the model setup.

Pressure and temperature gradients are established between the bottom of the storage formation at 20 MPa and 42ºC to atmospheric

pressure and temperatures. All models are run isothermally. The formation is uniformly given a salinity of 50,000 mg/L. Materials are given as "Aquifer I", "Aquifer II", and "Seal" in Table 2. Parameter values are determined from Birkholzer et al. (2008), Barnes et al. (2009), and Zhou et al. (2011) and are characteristic of the regional geology surrounding target storage formations. Injection rates match those of the homogeneous case at 160 Mt/yr of CO_2. Monitoring time is extended to an 80-year period following injection.

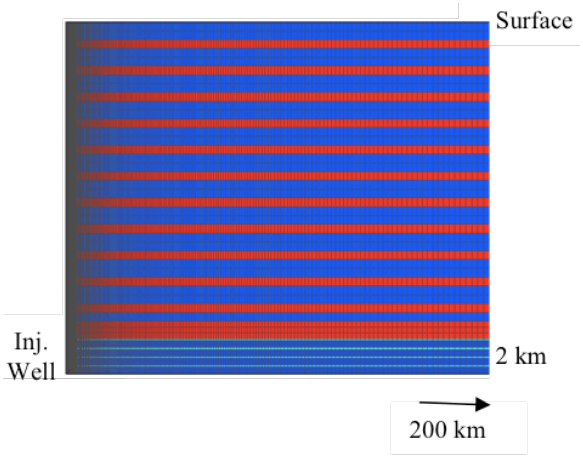

Figure 3. Setup of the stacked formation radial model. "Aquifer I" is given in dark blue, "Aquifer II" in light blue, and confining layers in red. Not to scale.

Results

Figure 4 shows the CO_2 front at the end of a 20-year injection period. The farthest the supercritical CO_2 travels from the well is 400 m. The plume is divided between the four layers of more permeable aquifer material, enhancing the pore volume utilized from the homogeneous case. The dissolved CO_2 travels 1,150 m.

Maximum pressures are achieved at the end of injection in gridblocks along the top of the storage formation closest to the well. These pressures are determined without considering brine production wells elsewhere in the target region. In the supercritical case, the largest pressure increase is 0.86 MPa; in the dissolved case, it is at 10.1 MPa.

Extents of pressure effects are again determined with a cutoff at 10.0 kPa in the vertical and horizontal directions. In the supercritical case, relevant pressure elevations are observed up to 50 m above the storage formation. Laterally, pressure elevations are observed up to 39.5 km from the injection well. In the dissolved case, pressure elevations are observed up to 125 m above the storage formation and up to 84 km radially from the injection well.

Table 2. Hydrogeologic properties of the stacked formation.

Property	Aquifer I	Aquifer II	Confining layers
Porosity	0.17	0.17	0.15
Horizontal permeability	100.0 md	1.0 md	1.0 x10^{-3} md
Vertical permeability	10.0 md	0.1 md	1.0 x10^{-4} md
Pore compressibility	3.71 Pa^{-1}	3.71 Pa^{-1}	7.42 Pa^{-1}
Relative permeability parameters			
Residual brine saturation	0.3	0.3	0.4
Van Genuchten parameter	0.41	0.41	0.41
Max. residual CO_2 saturation	0.25	0.25	0.3
Capillary pressure parameters			
Capillary entry pressure	4x10^3 Pa	4x10^3 Pa	5x10^6 Pa
van Genuchten parameter	0.41	0.41	0.41

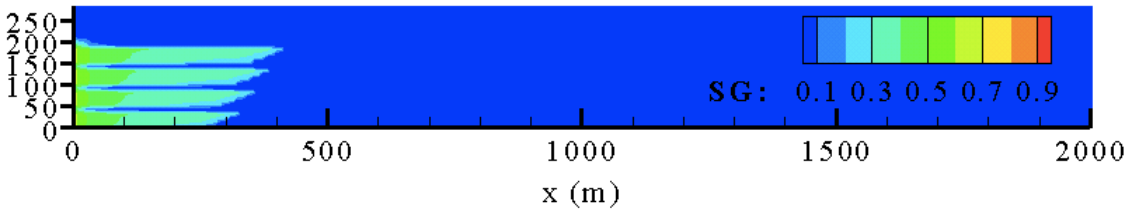

(a) Supercritical CO_2

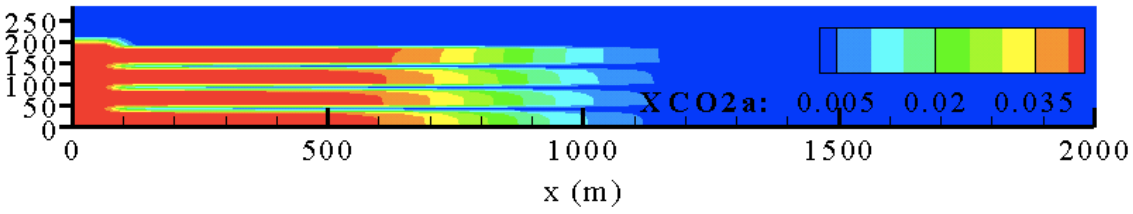

(b) Dissolved CO_2

Figure 4. The top cross section shows the radial distribution of supercritical CO_2 saturation after 20 years of injection. The bottom cross section shows distribution of the mass fraction of CO_2 after 20 years of injection in a dissolved phase.

Figure 5 shows the mobility of CO_2 after 80 years from the end of injection. The supercritical CO_2 travels along the borders of less permeable layers up to 500 m from the well. The less permeable "Aquifer II" layers within the storage aquifer act as barriers to the sinking dissolved CO_2. In 80 years, the dissolved CO_2 does not appreciably migrate.

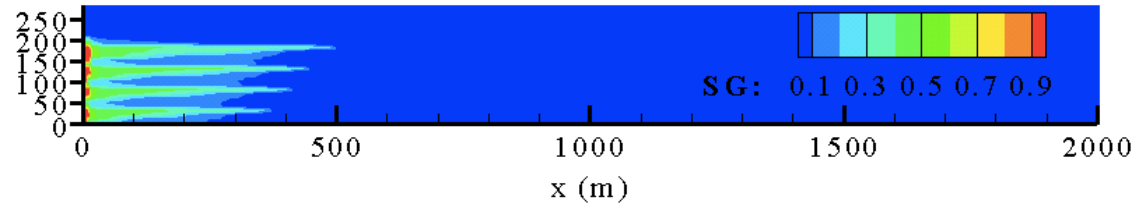

(a) Supercritical CO_2

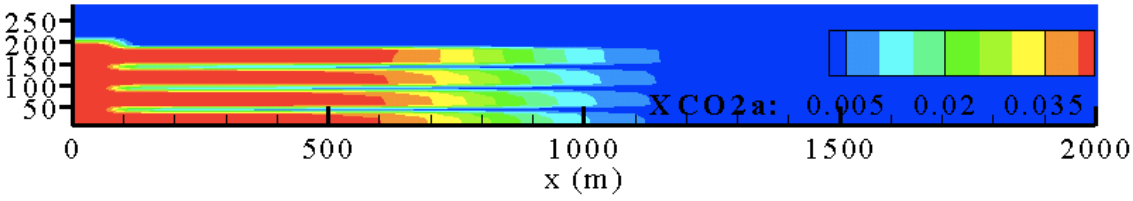

(a) Dissolved CO_2

Figure 5. The top cross section shows the radial distribution of supercritical CO_2 saturation 80 years after CO_2 injection stops. The bottom shows distribution of the mass fraction of CO_2 injected in a dissolved phase.

HETEROGENEOUS FORMATION

A heterogeneous permeability distribution within a storage formation reduces sweep efficiency in both supercritical and dissolved CO_2 injection schemes and may lower storage security (Tao and Bryant, 2012).

Model Setup

A regional scale model is constructed using a 200 km square, 2 km thick Voronoi grid. Within the 200 m thick storage formation, at the base of the model, is a zone surrounding the injection well containing heterogeneous, random, spatially correlated permeability fields. This zone is 10 km in radial extent from the well and is designed to encompass the CO_2 plume in either phase.

Lawrence Berkeley National Lab's iTOUGH2-GSLIB is used to generate these heterogeneous permeability fields. Using parameters similar to Barnes et al. (2009), the intrinsic permeability is given a log-normal distribution with a variance of 2.0 about an average permeability of 100 md. Sequential Gaussian Simulation is used to create a spherical variogram model with a vertical range of 1 m for log permeability. A long horizontal-to-vertical ratio of 10,000:1 is assumed for the variogram length.

Outside of the highly heterogeneous region, the storage formation is homogeneous. Above the storage formation, the model is set up as in the stacked case, alternating aquifers and confining units. Material properties match "Aquifer I" and "Confining layers" given in Table 2. Pressure and temperature gradients are established between the bottom of the storage formation at 20 MPa and 42ºC to atmospheric pressure and temperatures. All models are run isothermally. The formation is uniformly given a salinity of 50,000 mg/L. Injection rates and monitoring periods match those of the stacked cases.

Results

Figure 6 shows areal contours of the CO_2 plumes along the top of the storage formation and isosurface contours within the formation at the end of a 20-year injection period. The farthest the supercritical CO_2 travels from the well is 800 m. The farthest extent of the dissolved phase CO_2 is 1,750 m. The plume shape is largely determined by the permeability distribution, as is seen from the isosurface plots.

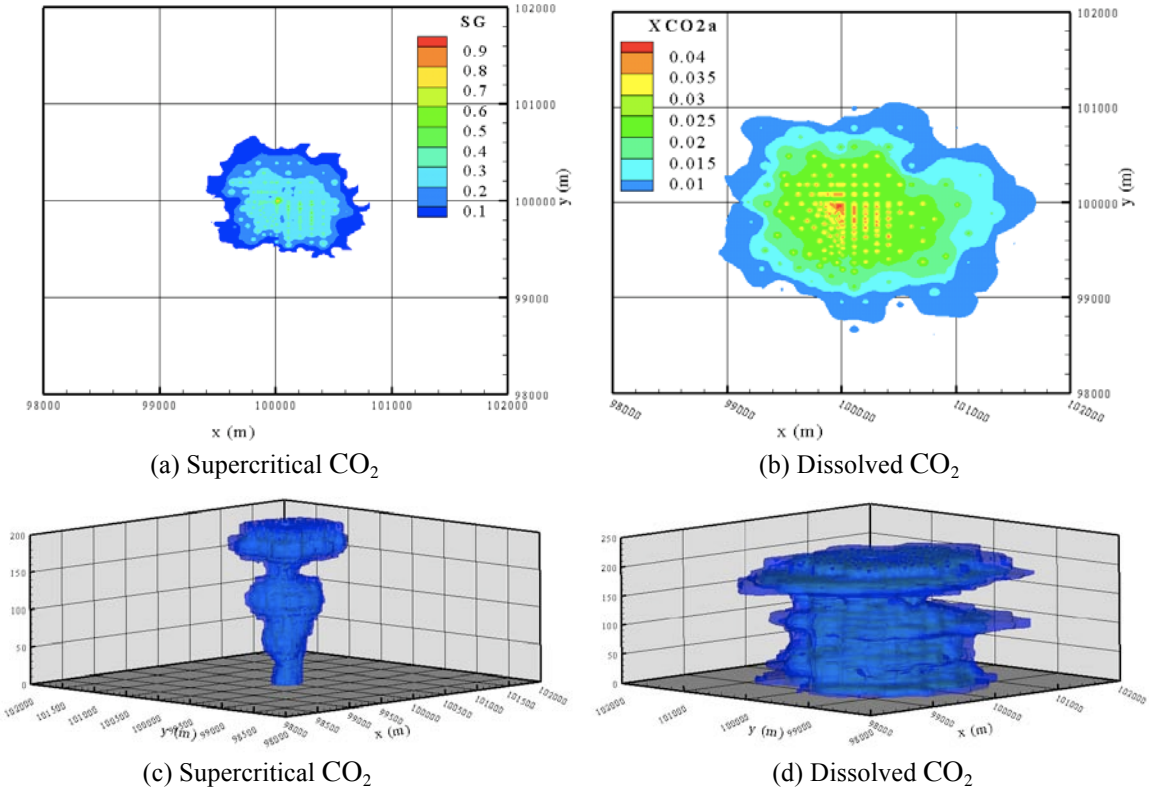

(a) Supercritical CO_2 (b) Dissolved CO_2

(c) Supercritical CO_2 (d) Dissolved CO_2

Figure 6. CO_2 distribution in the heterogeneous region of the storage formation after 20 years of injection (a) Areal cross section of supercritical CO_2 saturation. (b) Areal cross section of the mass fraction of dissolved CO_2. (c) 3-D isosurface of supercritical CO_2 saturation. (d) 3-D isosurface of the mass fraction of CO_2 in the aqueous phase.

Maximum pressures are achieved at the end of injection in gridblocks along the top of the storage formation closest to the well. These pressures are determined without considering brine production wells elsewhere in the target region. In the supercritical case, the largest pressure increase is 0.44 MPa; in the dissolved case, it is 72.3 MPa.

Extents of pressure effects are determined with pressure increase cutoff at 10.0 kPa in the vertical and horizontal directions. In the supercritical case, relevant pressure elevations are observed up to 50 m above the storage formation. Laterally, pressure elevations are observed up to 38.5 km from the injection well. In the dissolved case, relevant pressure elevations are observed up to 125 m above the storage formation. Laterally, pressure elevations are observed up to 89 km from injection well.

Figure 7 shows the mobility of CO_2 80 years from the end of the injection. The supercritical CO_2 remains highly mobile, traveling through high permeability lenses up and along the cap rock out to 1,000 m. The less permeable lenses within the storage aquifer act to immobilize dissolved CO_2. In 80 years, the dissolved CO_2 does not increase in maximum areal extent.

CONCLUSIONS

In this study, comparisons of migration and immobilization of CO_2 were made between supercritical CO_2 and CO_2-saturated brine injection strategies. Results show the initial areal footprint of supercritical CO_2 is less than half the size of the dissolved CO_2 in any formation heterogeneity. Following injection, supercritical CO_2 remains highly mobile, buoyantly flowing upward and extending outwards along the seal at least 20% radially. Dissolved CO_2 slowly sinks, essentially immobilized following injection. Additionally, dissolved CO_2 distributes more uniformly throughout the storage formation in cases of simple and complex formation heterogeneities.

Maximum pressure elevations are calculated without relief from production wells and are shown to be an order of magnitude greater for the dissolved CO_2 strategy in all cases. Vertical and horizontal pressure elevations due to dissolved CO_2 injection are observed to be between 2 and 2.5 times greater than supercritical pressure elevations.

These results indicate dissolved CO_2 injection enhances CO_2 trapping following injection and reduces the potential for unwanted release from storage. A larger volume is utilized for storage based on the properties of flow and total mass injected, requiring appropriate management of pressure elevations in targeted regions.

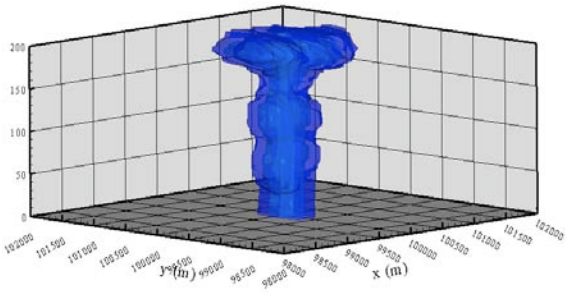

(a) Supercritical CO_2

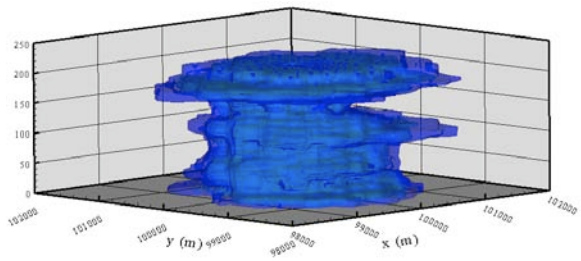

(b) Dissolved CO_2

Figure 7. CO_2 distribution in the heterogeneous region of the storage formation 80 years after injection ends (a) 3-D isosurface of supercritical CO_2 saturation. (b) 3-D isosurface of the mass fraction of CO_2 in the aqueous phase.

ACKNOWLEDGMENT

This research has been funded under U.S. EPA-STAR Grant #834383.

REFERENCES

Bachu, S., Sequestration of CO_2 in Geological Media in Response to Climate Change: Road Map for Site Selection using the Transform of the Geological Space into the CO_2 Phase Space, *Energy Conversion Management, 43*, 87 , 2002.

Barnes, D., D. Bacon, and S. Kelley., Geological Sequestration of Carbon Dioxide in the Cambrian Mount Simon Sandstone: Regional Storage Capacity, Site Characterization, and Large-Scale Injection Feasibility, *Environmental Geoscience,s 16*(3), 163, 2009.

Benson, S., et al. Underground Geologic Storage, *Intergovenmental Panel on Climate Change* Cambridge, U.K.: Cambridge University Press, 2005.

Birkholzer, J. T., and Z. Quanlin, Basin-Scale Hydrogeologic Impacts of CO_2 Storage: Capacity and Regulatory Implications, *International Journal of Greenhouse Gas Control*, *3*(6), 745-756, 2005.

Burton, M., and S. Bryant, Eliminating Buoyant Migration of Sequestered CO_2 through Surface Dissolution: Implementation Costs and Technical Challenges, SPE 110650, *2007 SPE Ann. Tech. Conf. Exhib.* Anaheim, CA. 2007.

Eke, P., M. Naylor, S. Haszeldine, A. Curtis, CO_2 -Brine Surface Dissolution and Injection: CO_2 Storage Enhancement, Publication SPE 124711, *Proceedings of the 2009 SPE Offshore Europe Oil & Gas Conference & Exhibition.* Aberdeen, UK. 2009.

Ennis-King, J. and L. Paterson, Engineering Aspects of Geological Sequestration of Carbon Dioxide, Publication SPE 77809, *Asia Pacific Oil and Gas Conference and Exhibition.* Melbourne, Australia. 2002.

Fang, Y., B. Baojun, T. Dazhen, S. Dunn-Norman, D. Wronkiewicz, Characteristics of CO_2 Sequestration in Saline Aquifers, *Pet. Sci., 7*, 83, 2010.

Garcia, J., K. Pruess, Flow Instabilities during Injection of CO_2 into Saline Aquifers, *TOUGH Symposium 2003,* Berkeley, California. 2003.

Hagoort, J., Fundamentals of Gas Reservoir Engineering, *Elsevier Science Publ.,* 23, 1988.

Jain, L. and S. L. Bryant, Optimal Design of injection/extraction wells for surface dissolution CO_2 storage strategy, *Energy Procedia,* 4, 4299-4306, 2011.

Lake, L. W., *Enhanced Oil Recovery*. NJ: Prentice Hall, 1989.

Leonenko, Y., D. Keith, Reservoir Engineering to Accelerate the Dissolution of CO_2 Stored in Aquifers, *Environ. Sci. Technol.* 42, 4742, 2007.

Tao, Q. and S. L. Bryant, Optimal Control of Injection/Extraction Wells for the Surface Dissolution CO_2 Storage Strategy, Carbon Management Technology Conference, 2012.

Yamamoto, H. and C. Doughty, Investigation of gridding effects for numerical simulation of CO_2 geologic sequestrations, *Int. Journal of Greenhouse Gas Control*, 2011.

Zhou, Q., J.T. Birkholzer, E. Mehnert, Y. Lin, K. Zhang, Modeling Basin- and Plume-Scale Processes of CO_2 Storage for Full-Scale Deployment, *Ground Water, 48*(4), 494-514, 2010.